Journal of GeoEngineering, Vol. 18, No. 2, pp. 059-069, June 2023
http://dx.doi.org/10.6310/jog.202306_18(2).2

NUMERICAL ANALYSIS OF SHAPE AND DEPTH FACTORS OF PERFECTLY ROUGH OR SMOOTH SHALLOW FOOTINGS ON AN INHOMOGENEOUS SINGLE LAYER OR INTERFACE OF TWO-LAYERED COHESIVE SOILS

Chao-Ming Chi [1*] and Zheng-Shan Lin [2]

ABSTRACT

This study utilizes an explicit finite difference program to investigate the effect of circular shape, embedment depth, and footing roughness to the bearing capacity of large shallow foundations placed on an inhomogeneous cohesive single layer soil deposit or set on the interface of a two-layered cohesive soil system. Because the dimensions of offshore foundations are in general larger than those of onshore footings, the inhomogeneous and layered soil effect to the bearing capacity would be more significant. Moreover, many large foundations are usually circular metal footings, such as spudcan footings of jack-up barges, so the considerations of shape and roughness effect are necessary. In this study, the soil is modelled by a perfectly plastic material with Tresca yield criterion and the associated flow rule. When a kinematically admissible velocity field which satisfies the constraints imposed by compatibility, velocity boundary and the flow rule is determined, the numerically collapse load can be obtained. The results from numerical simulations indicate that the bearing capacity is associated with the pattern of soil plastic flow and affected by the foundation shape, footing roughness, embedment ratio, soil strength ratio, and inhomogeneity factor. According to the numerical simulation results, several regression equations are recommended for the circular shape factor and depth factor with footing roughness consideration, so engineers can utilize those to fast calculate the bearing capacity of a footing on an inhomogeneous single layer soil deposit or a two-layered cohesive soil system. The results also indicate that even though the embedment depth benefits the bearing capacity, the effectiveness of stronger top soil layer is more significant because the associated soil plastic flow range enlarges.

Key words: Bearing capacity, large foundation, soil plastic flow, shape factor, depth factor, footing roughness.

1. INTRODUCTION

The important design considerations of shallow foundations include evaluating bearing capacity, installation resistance, and settlement (Randolph and Gourvenec 2011). Murff (2012) further indicated 'estimating foundation capacity has always been a central issue in foundation analysis and design'. In 1943, Terzaghi presented a comprehensive theory for the assessment of the ultimate bearing capacity (q_{ult}) of perfectly rough foundations (Das 2016). According to Terzaghi (1943), if a continuous foundation is placed on a homogeneous soil deposit, the ultimate bearing capacity (q_{ult}) can be expressed as

$$q_{ult} = cN_c + qN_q + 0.5B\gamma N_\gamma \tag{1}$$

where q_{ult} is the ultimate capacity, c is the cohesion in soil, q is surcharge, B is width of foundation, γ is the unit weight of soil, and N_c, N_q, and N_γ are bearing capacity factors. Additionally, the ultimate bearing capacity of a shallow foundation has been widely studied by a number of investigators such as Meyerhof (1951), Hansen (1970), and Vesić (1973), and Terzaghi's expression (Eq. (1)) is accepted to evaluate the bearing capacity. Hansen (1970) and Vesić (1973) indicated that while the foundation is placed in a homogeneous cohesive soil ($\phi' = 0$), the undrained bearing capacity can be written in the form

$$q_{ult} = S_u N_c (1 + s'_c + d'_c) + q \tag{2}$$

where S_u is the undrained shear strength, $N_c = \pi + 2$, which is equal to Prandtl's solution (Prandtl, 1921), s'_c is the shape factor and can be given by

$$s'_c = 0.2\frac{B}{L} \tag{3}$$

and d_c', the depth factor, can be expressed as

$$d'_c = \begin{cases} 0.4\times\dfrac{D_f}{B} & \text{for} \quad D_f / B \le 1.0 \\ 0.4\times\tan^{-1}\left(\dfrac{D_f}{B}\right) & \text{for} \quad D_f / B > 1.0 \end{cases} \tag{4}$$

where L is the length of foundation, and D_f is the depth of embedment of the foundation.

Manuscript received December 18, 2022; revised February 27, 2023; accepted April 12, 2023.

[1*] Assistant Professor (corresponding author), Department of Civil Engineering, Feng Chia University, Xitun Dist., Taichung, Taiwan (e-mail: cmchi@mail.fcu.edu.tw).

[2] Ph.D. Student, Program for Infrastructure Planning and Engineering, Feng Chia University, Xitun Dist., Taichung, Taiwan.

In reality, the undrained shear strength profile of cohesive soils usually does not satisfy the homogeneous condition. Under nature deposition conditions, the strength profile of cohesive soils might vary with depth (Chi and Lin 2020b). Skempton (1948) and Raymond (1967) reported that the self-weight of the soil causes a decrease in void ratio with depth, and this decrease often causes an approximately linear increase in strength with depth, particularly in normally-consolidated clays (Fig. 1). Raymond (1967), Reddy and Srinivasan (1971), Davis and Booker (1973), Chen (1975), Martin (2003), and Chi and Lin (2020b) applied the method of limiting equilibrium, the method of characteristics, upper bound method, or numerical simulations to assess the bearing capacity of the foundation placed on a single layer of inhomogeneous undrained cohesive soil (Fig. 1).

While a foundation is placed on a two-layered cohesive soils (Fig. 2), the associated bearing capacity might be affected by the normalized layer thickness (H/B) and strength ratio ($S_{u,\text{bot}}/S_{u,\text{top}}$) (Reddy and Srinivasan 1967; Brown and Meyerhof 1969; Chen 1975; Merifield *et al.* 1999; Chi and Lin 2020b), and the foundation failure mode might be less predictable. The Society of Naval Architects and Marine Engineers (SNAME) (2008) indicates that there are at least 3 difference basically different foundation failure modes which should be considered in in layered cohesive soils: (I) General shear failure occurs when $S_{u,\text{bot}}/S_{u,\text{top}} \approx 1.0$; (II) Squeezing

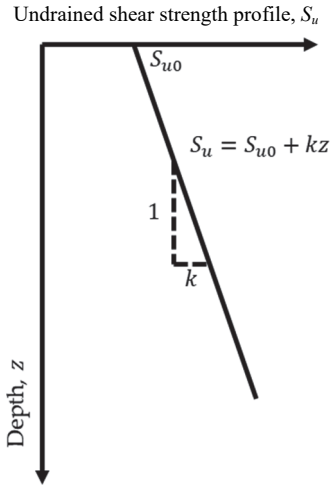

Fig. 1 Soil profile of the strength increasing with depth linearly

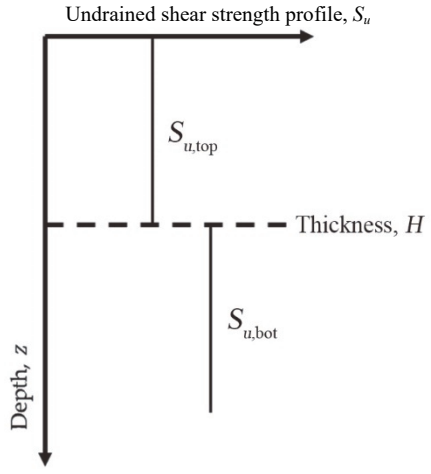

Fig. 2 Two-layered cohesive soil strength profile

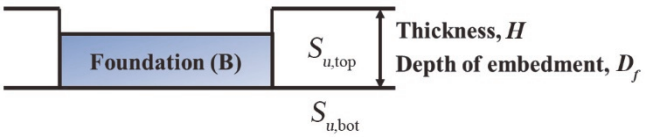

Fig. 3 Footing placed on the strata interface

might be considered if $S_{u,\text{bot}}/S_{u,\text{top}} > 1.0$. Although the stronger bottom stratum soil strength may contribute to the bearing capacity, the settlements may become more critical than capacity; (III) Punch-through failure must be of particular note and that usually accompany by a significant reduction in the bearing capacity if $S_{u,\text{bot}}/S_{u,\text{top}} < 1.0$. Hence, instead of a footing constructed on a relatively thin top stratum of two-layered system condition, engineers obtain more reliable bearing capacity evaluations of the footing placed on the strata interface, $D_f = H$ (Fig. 3).

2. PROBLEM DEFINITION

The purpose of this study is to investigate the effects of footing roughness and the shape of foundations to the ultimate bearing capacity of a foundation on a single layer of inhomogeneous undrained cohesive soil with strength increasing with depth (Fig. 1) and placed on the strata interface of the two cohesive soil layers (Fig. 2). This paper utilizes the numerical modeling software FLAC (Itasca 2019), Fast Lagrangian Analysis of Continua, to obtain the plastic collapse load.

The common diameter range for spudcan footings of jack-up barges is from 10 to 16m (Gütz 2012) and the rate of increase of undrained strength with depth (k) typically varies between 0 and 2 kPa/m (Hossain and Randolph 2010). In addition, Wang and Hwang (2022) provided the field investigation organizational data based on the in-situ CPT results at the western waters of Taiwan. Based on their results, the Best Estimated (BE, $S_{u\text{-BE}} = 26.5 + 2.335z$ kPa) and Upper Bound (UB, $S_{u\text{-BE}} = 50 + 5.385z$ kPa) strength profiles of cohesive soils, therefore, is suggested. Although the strength gradient (k) is higher, the seafloor strength (S_{u0}) is also higher leading to a relatively small value of the inhomogeneity factor (kB/S_{u0}). For example, considering a footing with diameter 20-m, the inhomogeneity factors computed from both profiles (*ie.,* $(kB/S_{u0})_{\text{BE}} = 2.335 \times 20/26.5 = 1.76$ and $(kB/S_{u0})_{\text{UB}} = 5.385 \times 20/50 = 2.15$) are within the range $0.0 \le kB/S_{u0} \le 3.0$. Hence, the recommended range of the inhomogeneity factor (kB/S_{u0}) is between 0.0 and 3.0 for most practical engineering and the associated soil parameters are also imposed in FLAC simulations. On the other hand, while the foundation is placed on the strata interface of the two cohesive soil layers, the properties applied in numerical models are $0.0 \le H/B = D_f/B \le 3.0$ and $0.2 \le S_{u,\text{bot}}/S_{u,\text{top}} \le 2.0$.

3. NUMERICAL SIMULATION

This study utilizes an explicit finite difference program to estimate the ultimate bearing capacity of a foundation. Figure 4 illustrates the general calculation sequence embodied in FLAC. The procedure first invokes the equations of motion to derive new velocities and displacements from stresses and forces; and then the strain rates are derived from velocities, and the new stresses from strain rates (Itasca 2019).

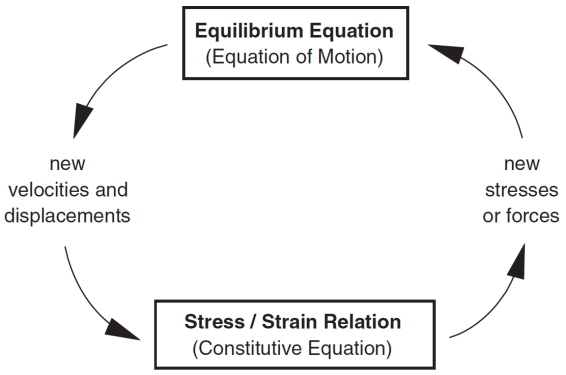

Fig. 4 Basic explicit calculation cycle (from Itasca 2019)

The shape of foundations considered in this study includes strip and circular footings, so the plane strain or axisymmetric condition with Tresca yield criteria is applied in the numerical simulations, and each of the boundary distances in the vertical and horizontal directions is 16*B* (Fig. 5). In addition, this study also investigates the footing roughness effect to ultimate bearing capacity. For perfectly rough footings, the strength along the foundation-soil-interface can be fully mobilized so there is no any relative sliding. On the other hand, the 0 of degree of mobilization of strength along the foundation-soil-interface is adopted.

In the nurmerical model, a downward velocity is imposed to the area representing the footings and the value of the velocity applied to the footing area is small enough to minimize any inertial effects. The soil reaction forces at footing grid points increases as the vertical displacement of the footings increases until reaching the numerical collapse load under the steady plastic flow condition. Therefore, the ultimate bearing capacity can then be obtained, Fig. 6.

To verify the results obtained in this study, the bearing factors and the associated velocity fields of a perfectly rough and a perfectly smooth strip footing on homogeneous cohesive materials under numerical limit load would be compared to the exact solutions estimated by Prandtl (1921) and Hill (1998). Furthermore, the bearing factor from the numerical simulation is either approximately 0.6% higher than the exact solution (Prandtl's mechanism) or about 0.8% below the exact solution

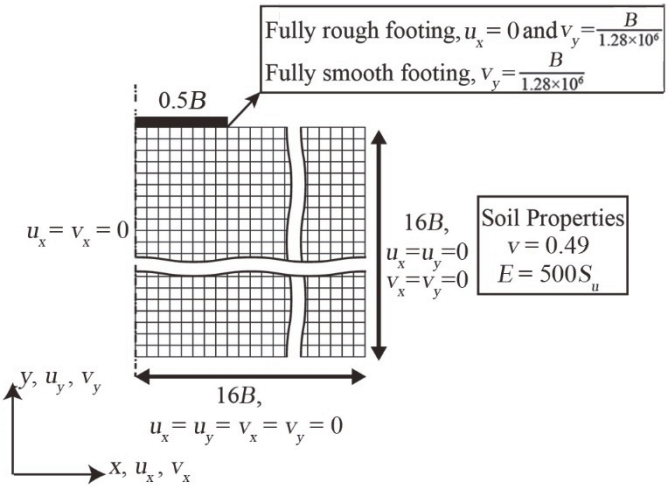

Fig. 5 Numerical simulation model

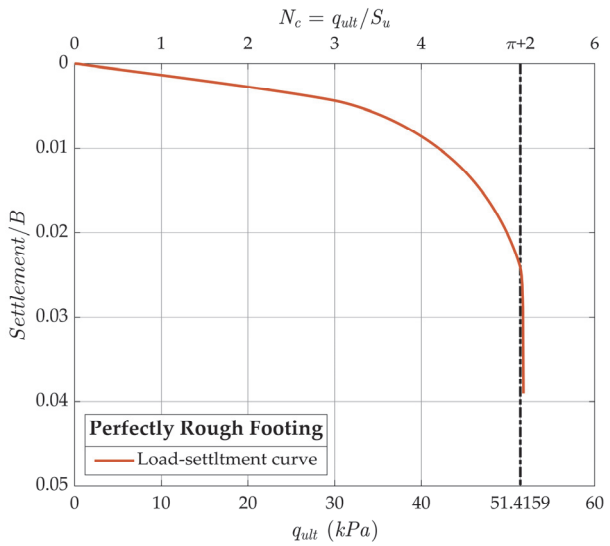

Fig. 6 Load-settlement curve of surface footings on homogeneous undrained deposits

(Hill's mechanism). Therefore, the good agreement with the exact solutions provides confidence in the accuracy of the numerical simulation results, so the results of the parametric study covering a wide range of soil properties and geometry can be discussed.

4. RESULTS AND DISCUSSION

4.1 Footings on a Single Layer of Inhomogeneous Cohesive Soil

The issue about the ultimate bearing capacity (Eq. (3)) of a footing placed on inhomogeneous cohesive single layer soil has been investigated by a number of researchers. Davis and Booker (1973) applied the method of characteristics to obtain the rigorous plasticity solutions for the bearing capacity of perfectly rough and perfectly smooth strip foundations. Martin (2003) used numerical implementations of the method of characteristics and the outcome solutions represent incomplete lower bound collapse loads. Raymond (1967), Reddy and Srinivasan (1971), Chen (1975), and Chi and Lin (2020b) calculated upper bound solutions assuming a simple circular failure surface. Furthermore, Chi and Lin (2020b) also provided the results of a perfectly rough and smooth strip foundation from FLAC, and the results will be discussed in this study.

The ultimate bearing capacity of a foundation placed on a cohesive medium can be expressed as (Hansen 1970)

$$q_{\text{ult}} = N_c(1+s_c')\,S_{u0} \tag{5}$$

where the shape factor is $s_c' = 0$ for strip footings and $s_c' = 0.2$ for circular footings. The bearing factors of a foundation on cohesive soils with the undrained shear strength with the depth (Fig. 1) is given in Fig. 7. It can be seen from this figure that: (I) to both strip and circular footings, the bearing factor increases as the inhomogeneity factor (kB/S_{u0}) increases; (II) for inhomogeneity factor $kB/S_{u0} < 2.25$, the bearing factor of circular footing is greater than that of strip footing; once inhomogeneity factor $kB/S_{u0} < 2.25$, the result is reversed; (III) the bearing factor is also affected by the footing roughness, and the inhomogeneity value of the intersection

of strip and circular footing curves is around 2.25 for both rough and smooth foundations. Figs. 8(a) and 8(b) demonstrate the effect of footing roughness to the bearing factor of strip and circular footings, respectively, and both FLAC simulation and Martin (2003) show the same trend but the difference increases as the inhomogeneity factor (kB/S_{u0}) increases. Compared with circular footing, the footing roughness effect to strip footing is less distinct for homogeneous soil condition ($kB/S_{u0} = 0$), but it becomes around 16% and 13% for FLAC and Martin, respectively, for both two shapes when inhomogeneity factor $kB/S_{u0} = 3$. It is notable that since the results from FLAC is based on the upper-bound method, applying a downward velocity on the footing, the associated bearing factors are expected to be larger than those from Martin using incomplete lower-bound method.

The bearing factor of circular footing on homogeneous soil is determined based on that of strip footing with the correction of shape factor (s_c'), and this approach is also adopted for a footing on soil with strength increasing as depth. In general, the shape factor is affected by the footing aspect ratio as well as soil friction angle. Moreover, the shape factor of a circular footing on homogeneous cohesive soil is $s_c' = 0.2$, according to Hansen's equation, so it implies that the shape effect benefits the bearing capacity of a circular footing when $kB/S_{u0} = 0$. Nevertheless, the shape factor is not always positive for circular footings on all soils. Figure 10 illustrates that the shape factor of circular footings on a cohesive soil with strength increasing as depth, and the differences between FLAC and Martin are tiny, especially for the rough footing. Both two methods indicate that the trend of the shape factor decreases as the inhomogeneity factor (kB/S_{u0}) increases, and it turns from positive to negative at around $kB/S_{u0} = 2.1$ and 2.25 for rough and smooth footings, respectively. The bearing factor of circular rough footing varies from 0.18 to −0.023 ($-0.023 \le s_c' \le 0.18$), within the inhomogeneity factor range $0 \le kB/S_{u0} \le 3$, so this variation range is wider than that of circular smooth footing ($-0.015 \le s_c' \le 0.11$). Therefore, it is not appropriate to use traditional shape factor to calculate the bearing capacity for large diameter foundations, such as offshore piles or spudcan footings of jack-up barges (Fig. 9), on soil with strength increasing as depth. Eqs. (6) and (7) are the regression forms of shape factors based on FLAC analysis for circular rough footings and smooth footings, respectively, so they are provided as fast calculation for large diameter footings.

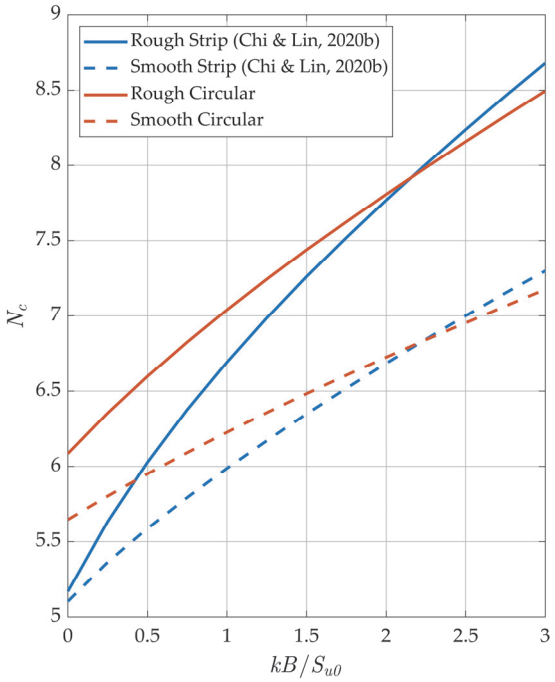

Fig. 7 Bearing capacity factors N_c

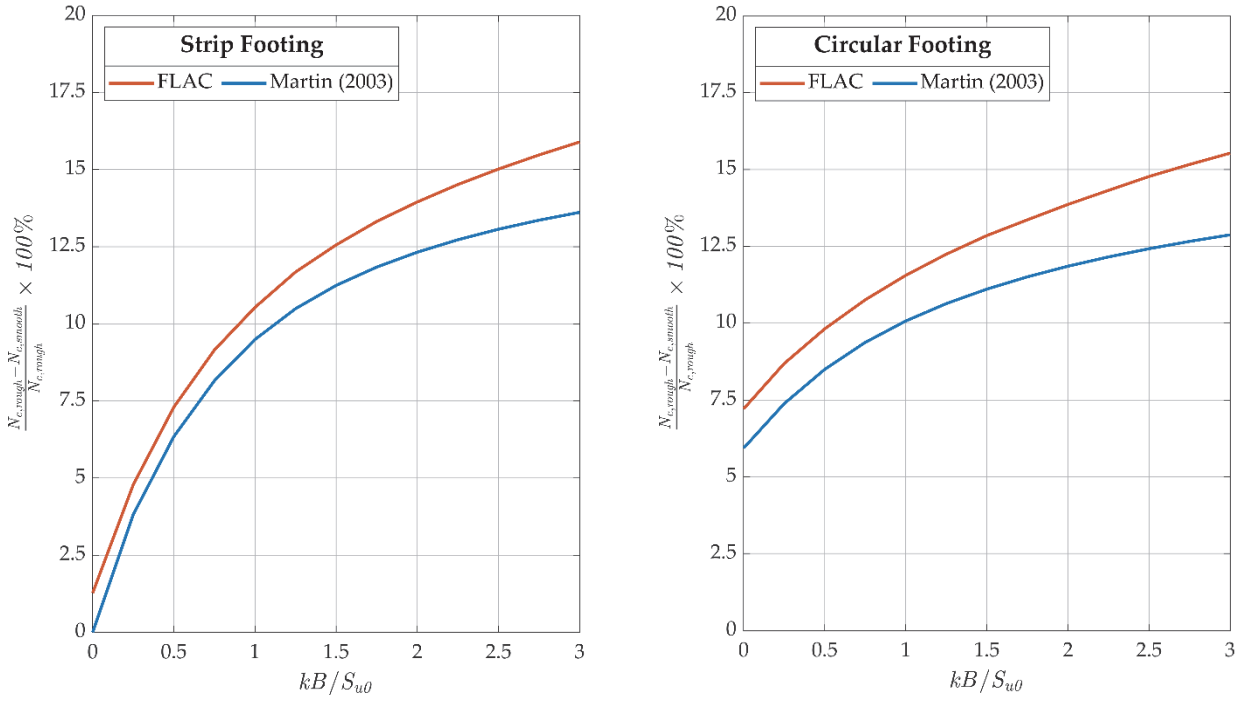

(a) Strip footing (b) Circular footing

Fig. 8 Effect of footing roughness to bearing factor

(a) Jack-up barge (from Durakovi 2020)

(b) Spudcan foundation (form Pisanò *et al.* 2019)

Fig. 9 View of jack-up barges and spudcan foundation

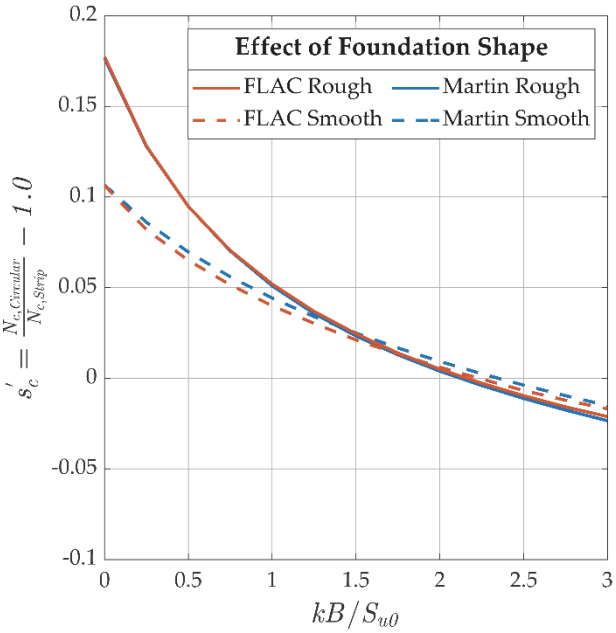

Fig. 10 Shape factor of circular footings on inhomogeneity soils

$$s'_{c,\text{rough}} = 0.06 \cot\left(0.24\frac{kB}{S_{u0}} - 2.89\right) - 0.06 \tag{6}$$

$$s'_{c,\text{smooth}} = 0.07 \cot\left(0.33\frac{kB}{S_{u0}} - 2.67\right) - 0.03 \tag{7}$$

4.2 A Foundation on the Interface of a Two-layered Cohesive Soil System

The in-situ soil is usually layered containing varieties of soil types, such as sand, silt, and clay, so the soil strength profile in general varies with depth varying (Chi and Lin 2022). In addition, the clayey silts exhibit the undrained behavior during rapid shear, and they could thus be regarded as cohesive soils in the assessment of foundation bearing capacity (Chi and Lin 2020a). Yang *et al.* (2006) indicated that there is often a relatively weaker cohesive soil layer with the thickness of about 5 meters at the ground surface in the southwest coastal area of Taiwan. If shallow foundations are constructed on a two-layered cohesive soil system, a thin weaker cohesive soil overlying a stronger cohesive soil, the primary problem would be settlements (Randolph and Gourvenec 2011). On the other hand, while shallow foundations are built on a strong layer overlying a weak layer, the punch-through failure accompanied by a rapid reduction in bearing capacity might occur. Hence, this is another option that is to place the foundations on the interface ($D_f = H$).

4.2.1 Evaluation of the Plastic Collapse Loads

Hansen (1970) suggested the undrained bearing capacity of a shallow foundation can be obtained by Eq. (2), and for a strip footing without a surcharge, this equation can be reduced to

$$q_{\text{ult}} = S_u N_c (1 + d'_c) \tag{8}$$

For the case of a two-layered cohesive soil system, Eq. (8) is rewrote in the form

$$q_{\text{ult}} = S_{u,\text{bot}} N_c (1 + d'^{*}_c) \tag{9}$$

where N_c is 5.17 and 5.10 purposed by Chi and Lin (2020b) obtaining from FLAC for a perfectly rough and smooth foundation, and $d_c'^{*}$ is a modified depth factor which is a function of D_f/B and $S_{u,\text{bot}}/S_{u,\text{top}}$.

The values of $d_c'^{*}$ are computed by numerical simulations from FLAC, and the results are shown in Figs. 11 and 12. According to Hansen (1970), Eq. (4), a piecewise function is used to determine the depth factor (d_c') of homogeneous cohesive soil condition. The value of d_c' increases from 0 to 0.4 linearly as the embedment ratio (D_f/B) increases, and it drops abruptly from 0.4 to $\pi/10$ at D_f/B = 1.0 and becomes a function of the arctangent. In brief, as the value of D_f/B increases, d_c' increases rapidly first and then slowly. The modified depth factor $d_c'^{*}$, affected by D_f/B and $S_{u,\text{bot}}/S_{u,\text{top}}$, is used to compute the ultimate bearing capacity of a strip foundation set on the interface of a two-layered cohesive soil system. If $S_{u,\text{bot}}/S_{u,\text{top}}$ remains the same, the value of $d_c'^{*}$ increases rapidly but slowly after $D_f/B > 0.25$. In addition, the $d_c'^{*}$ value decreases as $S_{u,\text{bot}}/S_{u,\text{top}}$ increases for the same D_f/B. The effect of the footing roughness is not beneficial, even diminished slightly, to the modified depth factor. For example, Eqs. (10) and (11) are the regression forms of the modified depth factor for rough and smooth footings, respectively, on $S_{u,\text{bot}}/S_{u,\text{top}}$ = 1.0 soil condition based on FLAC analysis, and the coefficient of the rough footing is smaller slightly.

$$d'_c = 0.3568 \times \tan^{-1}\left(\frac{D_f}{B}\right) \quad \text{for perfectly rough footings} \tag{10}$$

$$d'_c = 0.3684 \times \tan^{-1}\left(\frac{D_f}{B}\right) \quad \text{for perfectly smooth footings} \tag{11}$$

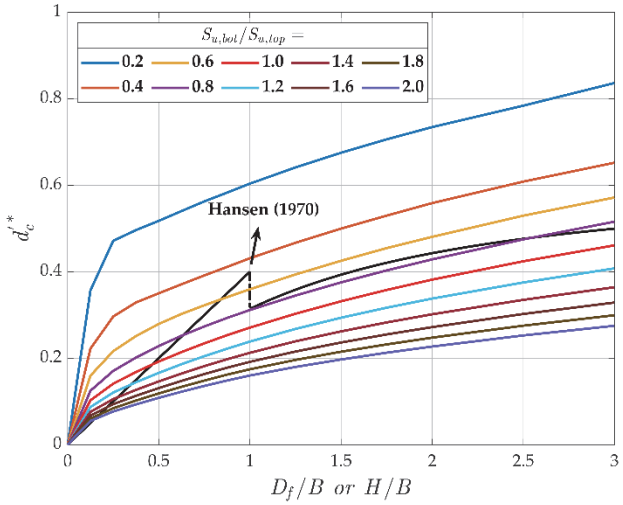

Fig. 11 Values of $d_c'^{*}$ for perfectly rough footings

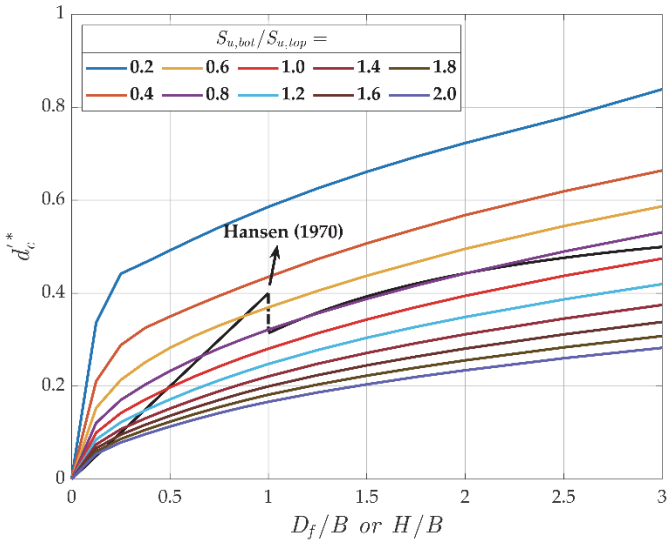

Fig. 12 Values of $d_c'^*$ for perfectly smooth footings

Prandtl (1921) was the first to purpose the failure mechanism, consisting of three different types of area, of the continuum due to a strip loading (Van Baars 2016). For a perfectly rough strip foundation with a constant downward velocity (v_0) placed on homogeneous cohesive soil ($\phi' = 0$), the numerical velocity field at the collapse loading and the associated Prandtl's mechanism are shown in Fig. 13(a), and the range of the field from FLAC is similar to the Prandtl's mode. Additionally, based on the upper bound theory, Chen and Han (1988) indicated the internal dissipation of energy occurs along line AB (triangle OAB is the active zone), arc BC, and line CD (triangle ACD is the passive zone), and in the region ABC (radial shear zone). Compared with the maximum shear strain rate shown in Fig. 13(b), where the internal dissipation of energy occurs matches where the value of shear strain rate is higher. Figure 14 illustrates the embedment depth effect to soil maximum shear strain rate of a footing on the interface of $S_{u,bot}/S_{u,top} = 1.0$ soil. It is obvious that for a small embedment depth ratio, such as $D_f/B = 0.25$ in Fig. 14(a), the foundation failure mode is close to Prandtl's mode. However, as the embedment depth ratio (D_f/B) increases, the length of soil failure surface and the range of the radial shear zone enlarge (Fig. 14(b)). The results imply that more energy dissipation in larger shear zone and longer slip surfaces, as D_f/B increasing, and lead to higher modified depth factor $d_c'^*$, as shown in Fig. 11.

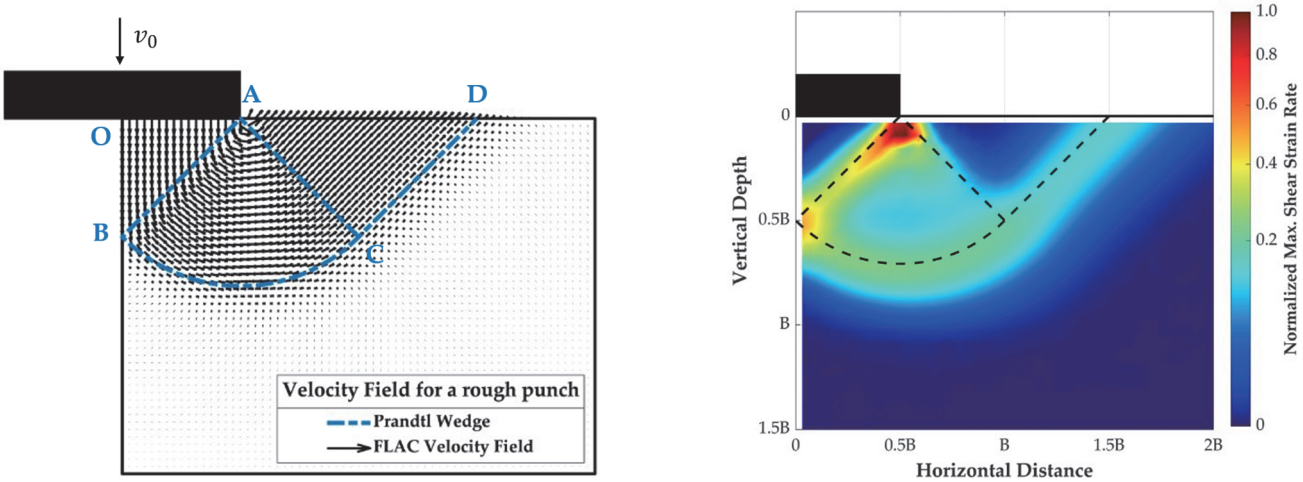

(a) Velocity field (b) Maximum shear strain rate

Fig. 13 Velocity field and maximum shear strain rate of a footing on a homogenous soil

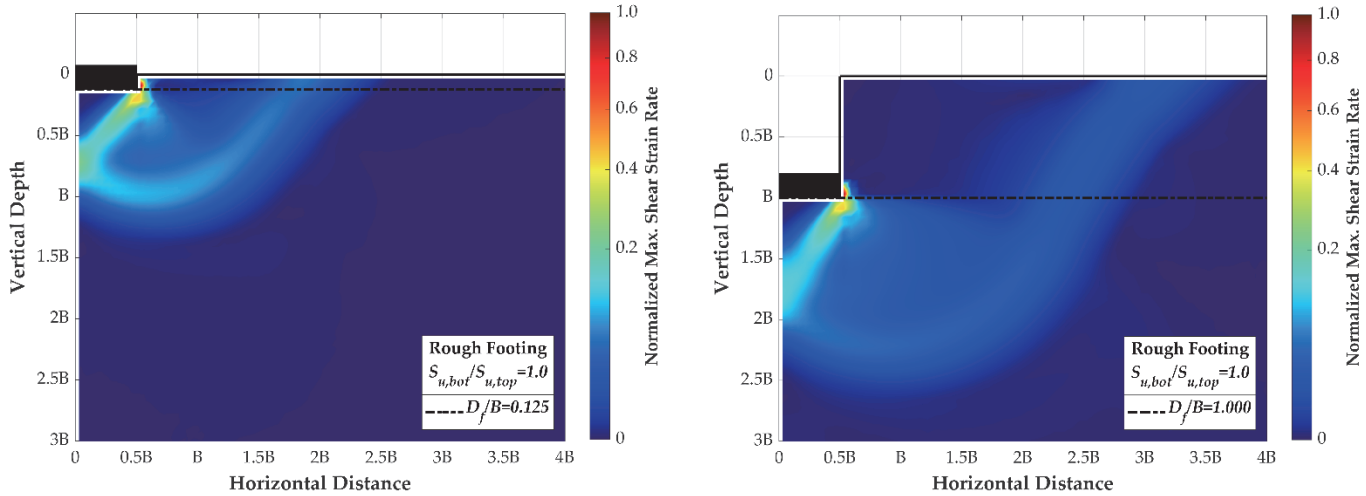

(a) $D_f/B = 0.125$ (b) $D_f/B = 1.0$

Fig. 14 Embedment depth effect to soil maximum shear strain rate

4.2.2 Footings on the interface of $S_{u,bot}/S_{u,top} \geq 1.0$ soils with shallow embedment

While foundations are set on an interface of two-layered cohesive soil system ($S_{u,bot}/S_{u,top} \geq 1.0$) with shallow embedment, such as $D_f/B \leq 1.0$ in Fig. 14, the soil failure surfaces extend to the ground surface and the associated failure mechanism is close to the characteristic of the general shear failure consisting of the active zone, radial shear zones, and passive zones. Figure 15 demonstrates the soil maximum shear strain rate of an embedment ratio $D_f/B = 0.5$ with various soil strength ratio: (I) the pattern and range of soil plastic flow are mainly affected by the embedment ratio D_f/B, compared with results in Fig. 14, rather than the soil strength ratio $S_{u,bot}/S_{u,top}$; (II) there exists a soil region (active zone) neighbor the foundation with the value of the maximum shear strain rate closing to 0.0 and it moves downward as a rigid body; (III) the dimension of the active zone is independent of the embedment ratio and the soil strength ratio; (IV) the value of maximum shear strain rate in the fan area (radial zone) decreases gradually from the border of the active zone to the passive zone, and the angle of the fan area increases as the embedment ratio increases.

As discussed in Section 4.2.1, the foundation bearing capacity is majorly affected by the embedment ratio (D_f/B) and the soil strength ratio ($S_{u,bot}/S_{u,top}$). Hence, the ultimate bearing capacity in $S_{u,bot}/S_{u,top} > 1.0$ side can be expressed as

$$\begin{aligned} q_{ult} &= S_{u,bot} N_c'^{*} \\ &= S_{u,bot} N_c (1 + d_c'^{*}) \\ &= S_{u,bot} N_c \left[(1 + d_c') + \frac{2}{N_c} \tan^{-1}\left(\frac{D_f}{B}\right)\left(\frac{S_{u,top}}{S_{u,bot}} - 1\right) \right] \end{aligned} \tag{12}$$

where $N_c = 5.17$ and d_c' can be obtained by Eq. (10) for perfectly rough footing, and $N_c = 5.10$ and d_c' can be determined from Eq. (11). The results of the ultimate bearing capacity (q_{ult}) of footings placed on the interface of a two-layered cohesive soils with $S_{u,bot}/S_{u,top} \geq 1.0$ conditions (Fig. 16) can be established by applying Eq. (12), and the error between Eq. (12) and numerical simulation from FLAC is less than 5.6%.

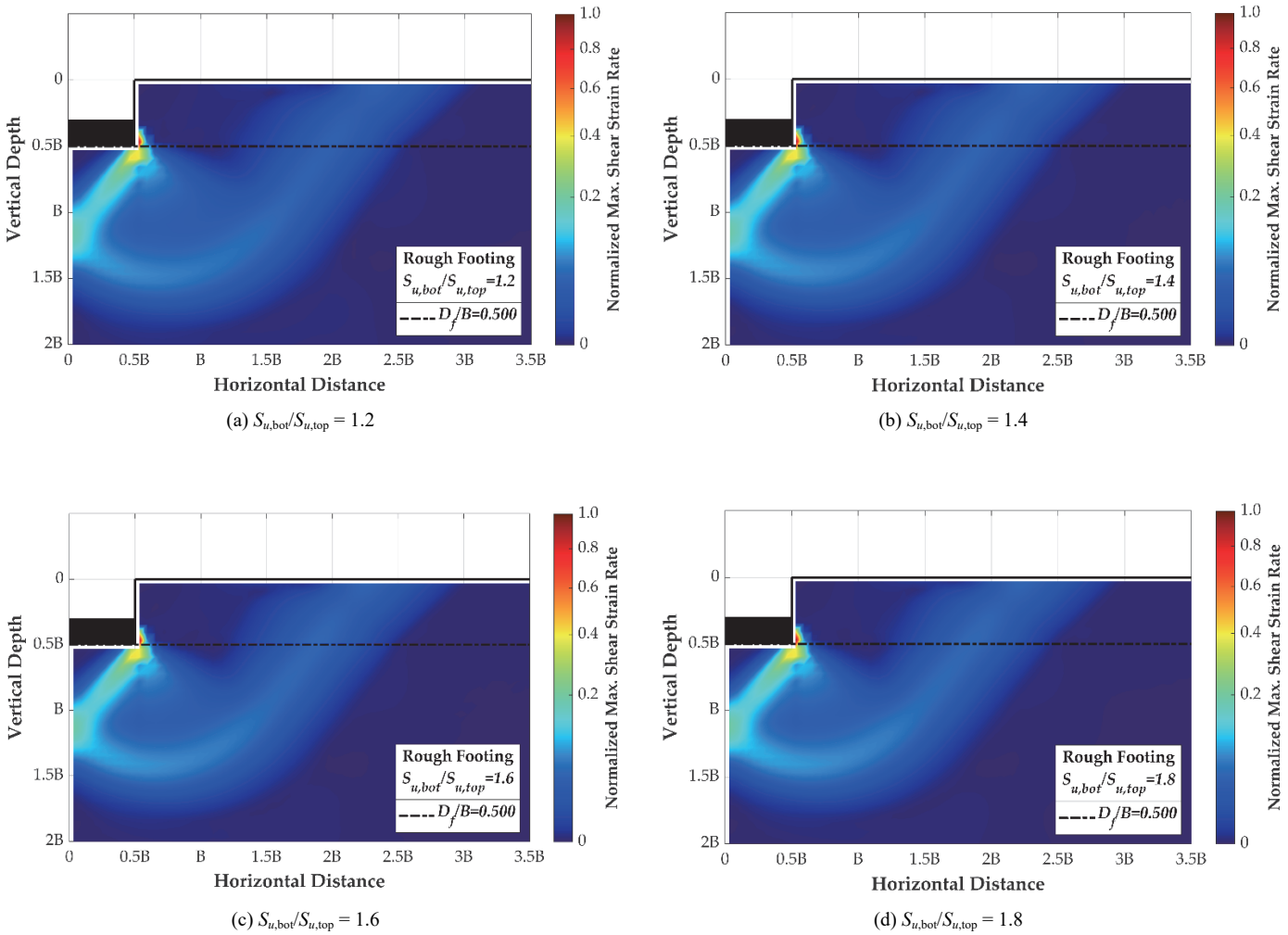

(a) $S_{u,bot}/S_{u,top} = 1.2$ (b) $S_{u,bot}/S_{u,top} = 1.4$

(c) $S_{u,bot}/S_{u,top} = 1.6$ (d) $S_{u,bot}/S_{u,top} = 1.8$

Fig. 15 Soil strength ratio effect to soil maximum shear strain rate

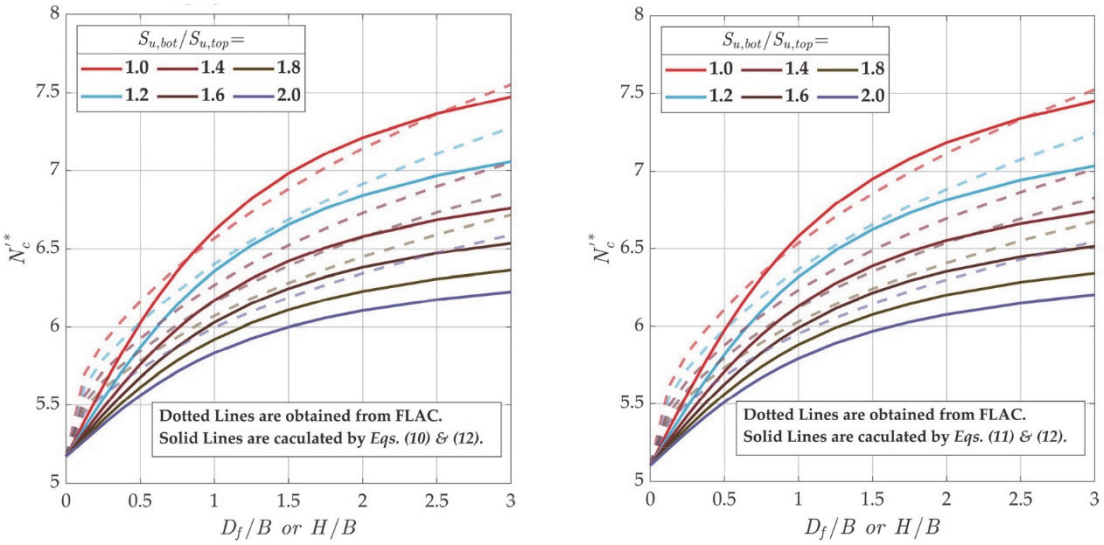

(a) Perfectly rough footing (b) Perfectly smooth footing

Fig. 16 Comparison of the results from Eq. (12) and FLAC

The general considerations for shallow foundations should include at least 3 different issues: prediction of installation resistance, evaluation of ultimate bearing capacity, and assessment of settlements (Randolph and Gourvenec 2011). The critical issue might be the settlements while foundations are placed on a soft cohesive soil layer overlying a strong layer ($S_{u,bot}/S_{u,top} \geq 1.0$). This type of the soil system ($S_{u,bot}/S_{u,top} \geq 1.0$) is very common in the southwest coastal area of Taiwan, where a weaker cohesive soil layer existed at a depth of about 5 meters below the ground surface (Yang *et al.* 2006). Hence, to avoid the issue of settlements, foundations can be directly set on the interface of a two-layered soils system with shallow embedment and then the evaluation of the associated ultimate bearing capacity should be implemented. However, the associated ultimate bearing capacity might be overestimated if the layered soil effect to the bearing capacity is neglected. For example, considering $H/B = D_f/B = 3.0$ and $S_{u,bot}/S_{u,top} = 2.0$, the associated ultimate bearing capacity could be established by using Hansen (1970) method (Eq. (4)) or the numerical results from FLAC (Fig. 11), and the difference is

$$\frac{q_{ult,Hansen} - q_{ult,FLAC}}{S_{u,bot}} = 1.12 \tag{13}$$

4.2.3 Footings on the interface of $S_{u,bot}/S_{u,top} < 1.0$ soils with shallow embedment

While foundations are placed on the interface with weaker bottom soil layer ($S_{u,bot}/S_{u,top} < 1.0$), the associated foundation failure mode is also affected by the embedment ratio and the soil strength ratio. Figures 17(a) and 17(b) show the soil velocity fields of a footing on the interface of a soil system with a shallow embedment ratio $D_f/B = 0.125$ and the strength ratio $S_{u,bot}/S_{u,top} = 1.0$ and 0.2, respectively, and Fig. 18 illustrates the maximum shear strain rate of the latter. Compared with Figs. 17(a) and 14(a), under the same embedment ratio $D_f/B = 0.125$, the following features are observed from Figs. 17(b) and 18: (I) the range of soil plastic flow is deeper and wider. In other words, the range of soil plastic flow enlarges as the soil strength ratio decreases; (II) the fan area in which the soil with rotational velocity revolves about a rotational origin in the top soil layer exists a greater value of the maximum shear strain rate. Furthermore, the rotational origin is in a local elastic zone nearby the footing edge; (III) the velocity vectors appear to be normal to the strata line and the passive zone vanishes in the bottom weaker layer. The values of maximum shear strain rate decrease from the border of the active zone to the soil strata line and drop dramatically on the interface. It seems that the top stronger layer constrains the upward development of soil plastic flow.

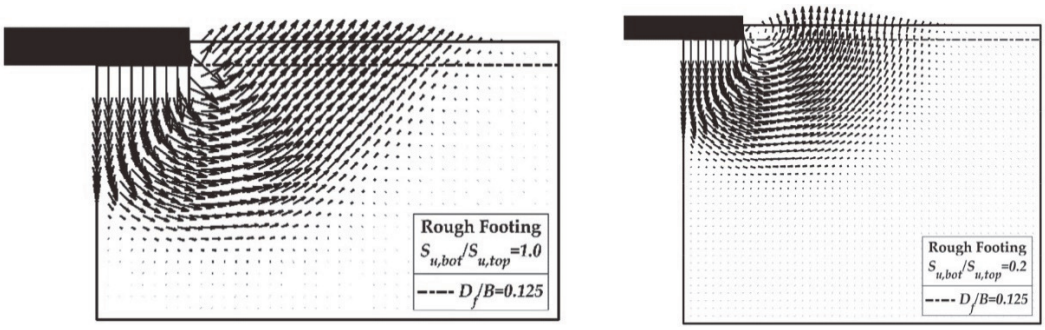

(a) $S_{u,bot}/S_{u,top} = 1.0$ (b) $S_{u,bot}/S_{u,top} = 0.2$

Fig. 17 Soil velocity field of rough footing with embedment ratio $D_f/B = 0.125$

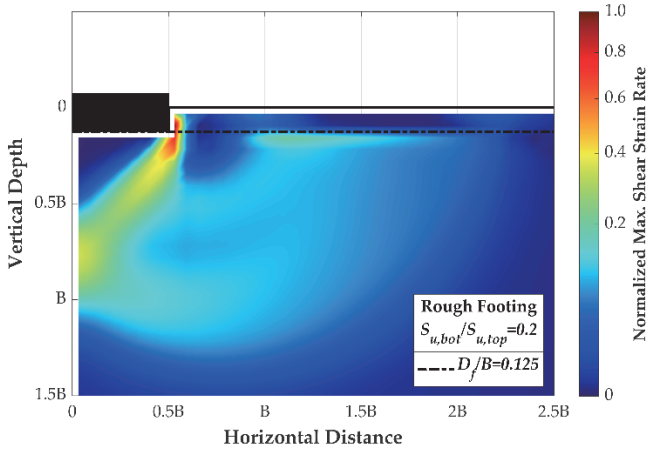

Fig. 18 Maximum shear strain rate field of rough footing with embedment ratio D_f/B = 0.125 and soil strength ratio $S_{u,bot}/S_{u,top}$ = 2.0

Das (2009) indicated the embedment ratio can be as larger as 3.0 to 4.0 for shallow foundations; therefore, the range of the embedment ratio, $0.0 \le D_f/B \le 3.0$ in Figs. 11 and 12, conducting in this study is representative for shallow footings. If the general shear failure occurs, it is expected that the failure surface in soil would extend to the ground surface for shallow footings on homogeneous soils. When a foundation on a two-layered soil system with higher strength of the top layer, the soil failure surface may not extend into the top layer or to ground surface, such as the results demonstrated in Fig. 19. With an embedment ratio D_f/B = 1, it is obvious that the soil plastic flow is constrained in the bottom weaker layer for both cases, and range of the flow of $S_{u,bot}/S_{u,top}$ = 0.4 is slightly larger than the other. It is worth mentioning that the range of soil plastic flow is proportional to the modified depth factor d_c^*, shown in Figs. 11 and 12, and the effectiveness of stronger top soil layer to footing bearing capacity is more than that of weaker top soil layer.

4.2.4 Roughness Effect

The roughness effect to the footing capacity is not significant (< 3.3%), and it is also related to the embedment ratio and soil strength ratio, demonstrated in Fig. 20. The roughness effect is beneficial to the bearing capacity, rather than modified depth factor discussed in the Section 4.2.1, and the following features can be found: (I) the maximum value is about 3.3%, around at $S_{u,bot}/S_{u,top}$ = 2.0 and D_f/B = 0.25, and the effect decreases as $S_{u,bot}/S_{u,top}$ and D_f/B increases; (II) for a surface footing (D_f/B = 0), the effect maintains at a constant about 1.3%; (III) if the soil strength ratio remains unchanged, the contribution of footing roughness to the bearing capacity decreases as the embedment ratio increases. Furthermore, the bearing capacity is unaffected by the footing roughness if the embedment ratio is large enough.

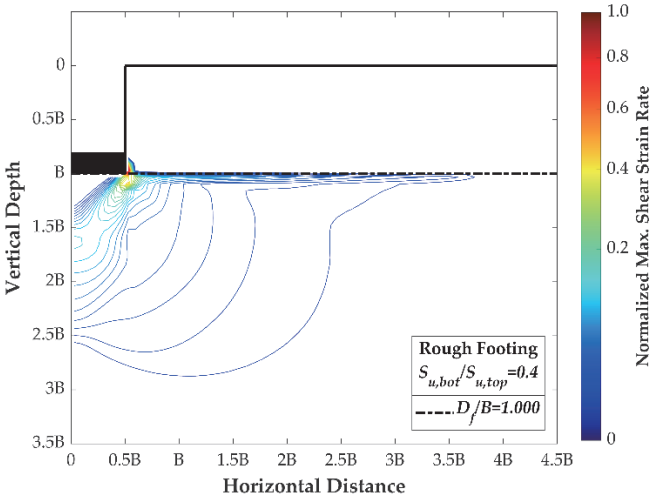

(a) $S_{u,bot}/S_{u,top}$ = 0.4

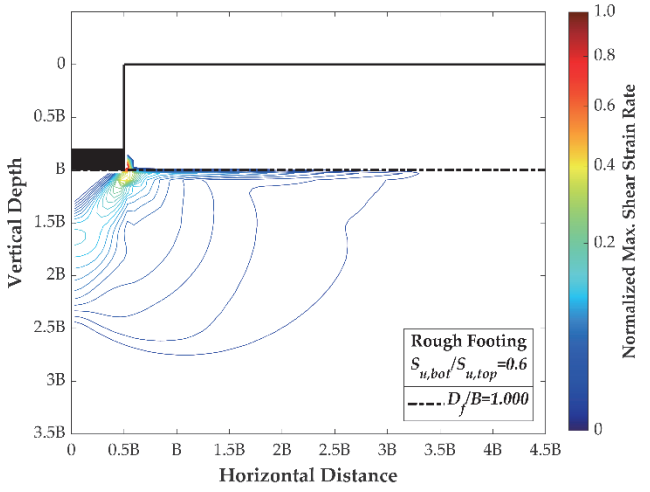

(b) $S_{u,bot}/S_{u,top}$ = 0.6

Fig. 19 Contours of the Maximum Shear Strain Rate of D_f/B = 1.0

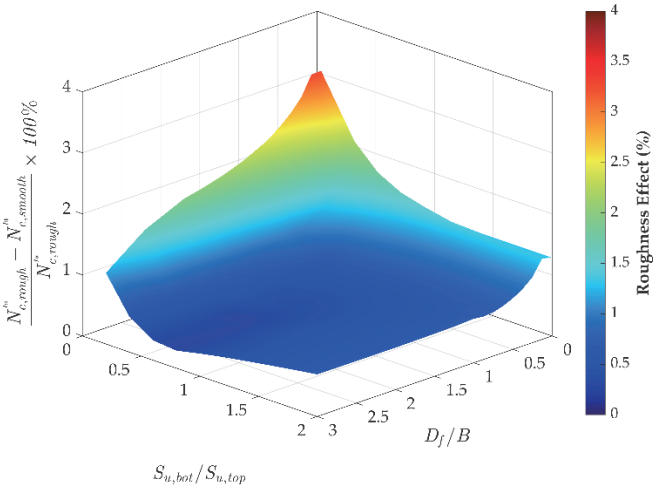

Fig. 20 Roughness Effect Surface

5. CONCLUSIONS

Foundations are the lowest components of structures and support a variety of buildings. To ensure that foundations can transmit the loads to the underlying soils, the issue of bearing capacity evaluation is the critical challenge for geotechnical engineers. The bearing capacity of foundations and the associated failure mechanism are in general affected by the dimension, shape, roughness, and embedment depth of foundations, inhomogeneity factor (kB/S_{u0}), and soil strength ratio ($S_{u,bot}/S_{u,top}$). This study utilizes the

numerical software to investigate the plastic collapse load of a foundation set on a single layer of inhomogeneous undrained cohesive soil with strength increasing with depth (Fig. 1) and placed on the strata interface of the two cohesive soil layers (Fig. 3). For the effects of the shape of foundations, footing roughness, and inhomogeneity factor (kB/S_{u0}) to the ultimate bearing capacity of a foundation on a single layer of inhomogeneous cohesive soil, the results and highlights are as follows:

1. To both strip and circular footings, the bearing factor increases as the inhomogeneity factor (kB/S_{u0}) increases. For inhomogeneity factor $kB/S_{u0} < 2.25$, the bearing factor of circular footing is greater than that of strip footing; once inhomogeneity $kB/S_{u0} > 2.25$, the result is reversed. For the effect of footing roughness to the bearing factor of strip and circular footings, the simulation results indicate that the footing roughness could contribute to the bearing capacity and the value of bearing factor would increase as the inhomogeneity (kB/S_{u0}) increases. In addition, compared with circular footing, the footing roughness effect to strip footing is less distinct for homogeneous soil condition ($kB/S_{u0} = 0$), but it becomes around 16% for both two shapes when inhomogeneity is $kB/S_{u0} = 3$.
2. The bearing capacity of circular footings can be evaluated from that of strip foundations by applying shape factor (s_c'). For a foundation placed on a homogeneous cohesive deposit, the bearing capacity of circular footings is always larger than that of strip foundations because the value of the shape factor is positive. However, the s_c' value would change from positive to negative as inhomogeneity (kB/S_{u0}) increases and it implies that the bearing capacity may be overestimated if the inhomogeneous soil effect is neglected. The useful regression forms (Eqs. (6) and (7)) of shape factors (s_c') based on the numerical simulation from FLAC for circular rough footings and smooth footings respectively are provided in this paper.

The plastically collapse load of footings on the interface of a two-layered cohesive soil system has been investigated in this study and the following conclusions can be draw:

1. Based on a series of numerical simulates, this paper provides the regression forms (Eqs. (10) and (11)) of the depth factor for respectively perfectly rough and smooth footings placed in homogeneous cohesive soils ($S_{u,bot}/S_{u,top} = 1.0$). While footings are set on the interface of $S_{u,bot}/S_{u,top} > 1.0$ soils with shallow embedment depth, the modified depth factor ($d_c'^*$) is always smaller than that of the homogeneous condition ($S_{u,bot}/S_{u,top} = 1.0$). Furthermore, if the embedment ratio (D_f/B) remains a constant value, the modified depth factor ($d_c'^*$) would decrease with $S_{u,bot}/S_{u,top}$ increasing. It implies, hence, that the bearing capacity of footings placed on the interface of $S_{u,bot}/S_{u,top} > 1.0$ soils might be less conservative if the layered soil effect is not included in the design considerations. It is worth mentioning that the patterns of soil plastic flow for all weaker top layer soils ($S_{u,bot}/S_{u,top} > 1.0$) are very similar and close to Prandtl's mode ($S_{u,bot}/S_{u,top} = 1.0$), in spite of the value of the soil strength ratio and embedment ratio. This article provides a brief equation (Eq. (12)) to evaluate the ultimate bearing capacity on $S_{u,bot}/S_{u,top} > 1.0$ side. Additionally, the pattern and range of soil plastic flow are mainly affected by the embedment ratio (D_f/B) rather than the soil strength ratio ($S_{u,bot}/S_{u,top}$).
2. Considering a footing on the interface of $S_{u,bot}/S_{u,top} < 1.0$ soils with shallow embedment depth, the modified depth factor ($d_c'^*$) is always greater than that of the homogeneous condition ($S_{u,bot}/S_{u,top} = 1.0$) and the $d_c'^*$ value increases as the embedment ratio (D_f/B) increases or the soil strength ratio ($S_{u,bot}/S_{u,top}$) decreases. The pattern of soil plastic flow is different with Prandtl's mode on $S_{u,bot}/S_{u,top} < 1.0$ side. The fan area of soil plastic flow in which the soil with rotational velocity revolves about a rotational origin in the top soil layer would enlarge and the rotational origin is in a local elastic zone nearby the footing edge, and the velocity vectors appear to be normal to the strata line and the passive zone vanishes in the bottom weaker layer. On the other hand, the range of the soil plastic flow is affected by the embedment ratio, and it enlarges as the embedment ratio decreases. It is worth mentioning that the effectiveness of stronger top soil layer to footing bearing capacity is more than that of weaker top soil layer.
3. The roughness effect to the footing capacity is not significant, and it is also related to the embedment ratio (D_f/B) and soil strength ratio ($S_{u,bot}/S_{u,top}$). Additionally, the roughness effect is beneficial to the bearing capacity, rather than modified depth factor.

ACKNOWLEDGEMENTS

This research presented here was supported by the grants: Investigations of ultimate bearing capacity and associated soil plastic flow of jack-up barge foundations in layered soils (MOST 111-2221-E-035-030) and The ultimate bearing capacity analysis of the mooring anchors of Taiwan offshore floating-type wind turbine platforms and the foundations of jack-up barges (MOST 110-2221-E-035-029-), the Ministry of Science and Technology of Taiwan.

FUNDING

This research was funded by the Ministry of Science and Technology (MOST) of Taiwan, grant number MOST 111-2221-E-035-030 and MOST 110-2221-E-035-029-.

DATA AVAILABILITY

The data and/or computer codes used/generated in this study are available from the corresponding author on reasonable request.

CONFLICT OF INTEREST STATEMENT

The authors declare that there is no conflict of interest.

NOTATIONS

B	width of foundation (L)
d_c'	depth factor
D_f	depth of embedment of the foundation (L)
D_f/B	embedment ratio
H	thickness of top layer (L)
H/B	normalized layer thickness
k	rate of increase of undrained strength with depth ($ML^{-2}T^{-2}$)

kB/S_{u0}	inhomogeneity factor
N_c, N_q, N_γ	bearing factors
ϕ'	soil friction angle
q_{ult}	ultimate bearing capacity ($ML^{-1}T^{-2}$)
γ	unit weight of soil ($ML^{-2}T^{-2}$)
s_c'	shape factor
S_u	undrained shear strength of cohesive soil ($ML^{-1}T^{-2}$)
S_{u0}	undrained shear strength of cohesive soil at the ground surface ($ML^{-1}T^{-2}$)
$S_{u,bot}$	undrained shear strength of bottom layer soil ($ML^{-1}T^{-2}$)
$S_{u,top}$	undrained shear strength of top layer soil ($ML^{-1}T^{-2}$)
$S_{u,bot}/S_{u,top}$	strength ratio

REFERENCES

Brown, J.D. and Meyerhof, G.G. (1969). *Experimental Study of Bearing Capacity in Layered Clays*. **2**, 45-51, Mexico City, Mexico: International Society for Soil Mechanics and Geotechnical Engineering.

Chen, W.-F. (1975). *Limit Analysis and Soil Plasticity*, Elsevier Scientific Pub. Co.

Chen, W.-F. and Han, D.J. (1988). *Plasticity for Structural Engineers*. Springer.

Chi, C.-M. and Lin, Z.-S. (2020a). "The footing size effect on punch-through bearing capacity assessment of jack-up barges in Western Taiwan Offshore Layered Soil." *The 30th International Ocean and Polar Engineering Conference*, ISOPE-I-20-2223, Shanghai, China: The International Society of Offshore and Polar Engineers.

Chi, C.-M. and Lin, Z.-S. (2020b). "The bearing capacity evaluations of a spread footing on single thick stratum or two-layered cohesive soils." *Journal of Marine Science and Engineering*, **8**(11), 853. https://doi.org/10.3390/jmse8110853

Chi, C.-M. and Lin, Z.-S. (2022). "An investigation of ultimate bearing capacity and associated plastic flow of a footing on the interface of weaker cohesive soil underlain by stronger cohesive soil." *Proceedings of the 19th Conference on Current Researches in Geotechnical Engineering*, A-04 (in Chinese with English abstracts).

Das, B.M. (2009). *Shallow Foundations: Bearing Capacity and Settlement*. CRC Press. http://www.crcnetbase.com/isbn/9781420070064

Das, B.M. (2016). *Principles of Foundation Engineering*. 8th Edition, Cengage Learning.

Davis, E.H. and Booker, J.R. (1973). "The effect of increasing strength with depth on the bearing capacity of clays." *Géotechnique*, **23**(4), Article 4. https://doi.org/10.1680/geot.1973.23.4.551

Durakovi, A. (2020). "Mega jack-up to officially debut on world's largest offshore wind farm." *Offshorewind*. https://www.offshorewind.biz/2020/08/07/mega-jack-up-to-officially-debut-on-worlds-largest-offshore-wind-farm/

Gütz, P. (2012). "Finite element analysis of spudcan footing penetration." Diploma Thesis, Leibniz Universität Hannover, Hannover, Germany. https://doi.org/10.13140/RG.2.2.18359.27047

Hansen, J.B. (1970). *A Revised and Extended Formula for Bearing Capacity*, Bulletin No. 28, Danish Geotechnical Institute.

Itasca Consulting Group, Inc. (2019). *FLAC—Fast Lagrangian Analysis of Continua*, Ver. 8.1. Minneapolis: Itasca.

Martin, C. (2003). "New software for rigorous bearing capacity calculations." *BGA International Conference on Foundations, Innovations, Observations, Design and Practice*, 581-592, Dundee, Scotland: British Geotechnical Association.

Merifield, R.S., Sloan, S.W., and Yu, H.S. (1999). "Rigorous plasticity solutions for the bearing capacity of two-layered clays." *Géotechnique*, **49**(4), 471-490. https://doi.org/10.1680/geot.1999.49.4.471

Meyerhof, G.G. (1951). "The ultimate bearing capacity of foundations." *Géotechnique*, **2**(4), 301-332. https://doi.org/10.1680/geot.1951.2.4.301

Murff, J.D. (2012). "Estimating the capacity of offshore foundations." *Offshore Site Investigation and Geotechnics: Integrated Technologies—Present and Future*. Inaugural McClelland Lecture, London, UK.

Pisanò, F., Schipper, R., and Schreppers, G.-J. (2019). "Input of Fully 3D FE Soil-structure Modelling to the Operational Analysis of Jack-Up Structures." *Marine Structures*, **63**, 269-288. https://doi.org/10.1016/j.marstruc.2018.09.011

Prandtl, L. (1921). "Hauptaufsätze: Über die Eindringungsfestigkeit (Härte) plastischer Baustoffe und die Festigkeit von Schneiden." *Journal of Applied Mathematics and Mechanics / Zeitschrift Für Angewandte Mathematik Und Mechanik*, **1**(1), 15-20. https://doi.org/10.1002/zamm.19210010102

Randolph, M.F. and Gourvenec, S. (2011). *Offshore Geotechnical Engineering*. Spon Press.

Raymond, G.P. (1967). "The bearing capacity of large footings and embankments on clays." *Géotechnique*, **17**(1), 1-10. https://doi.org/10.1680/geot.1967.17.1.1

Reddy, A.S. and Srinivasan, R.J. (1967). "Bearing capacity of footings on layered clays." *Journal of the Soil Mechanics and Foundations Division*, ASCE, **93**(SM2), 83-99. https://doi.org/10.1061/JSFEAQ.0000961

Reddy, A.S. and Srinivasan, R.J. (1971). "Bearing capacity of footings on clays." *Soils and Foundations*, **11**(3), 51-64. https://doi.org/10.3208/sandf1960.11.3_51

Skempton, A.W. (1948). "A study of the geotechnical properties of some post-glacial clays." *Géotechnique*, **1**(1), 1-16. https://doi.org/10.1680/geot.1948.1.1.1

SNAME (2008). "Guidelines for site specific assessment of mobile jack-up units." *Guidelines for Site Specific Assessment of Mobile Jack-Up Units* . T&R Bulletin 5-05 A, Rev. 2, Society of Naval Architects and Marine Engineers, New Jersey.

Terzaghi, K. (1943). *Theoretical Soil Mechanics*. John Wiley and Sons.

Van Baars, S. (2016). *100 Year Prandtl's Wedge Intermediate Report*. https://doi.org/10.13140/RG.2.2.18068.40324

Vesić, A.S. (1973). "Analysis of ultimate loads of shallow foundations." *Journal of the Soil Mechanics and Foundations Division*, ASCE, **99**(1), 45-73. https://doi.org/10.1061/JSFEAQ.0001846

Wang, J.-S. and Hwang J.-H. (2022). "A comparative study on the calculation methods of axial bearing capacity of foundation piles for offshore wind turbines: (II) Marine soils." *Sino-Geotechnics*, 174 (in Chinese with English abstract).

Yang, Z.-Y., Chen, C.-S., Zhu, J.-Y., and Lai, R.-Y. (2006). "The distribution of soft soils in the southwestern coastal area of Taiwan." *Proceedings of the Design Procedures of Traffic Structures on the Soft Soil Foundation Located in the Southwestern Coastal Area of Taiwan*, **1**, 1-18, Taichung, Taiwan: Institute of Transportation, MOTC (in Chinese).